

Phase-matched four-wave mixing and sensing of water molecules by coherent anti-Stokes Raman scattering in large-core-area hollow photonic-crystal fibers

Stanislav O. Konorov, Andrei B. Fedotov, and Aleksei M. Zheltikov

Department of Physics, International Laser Center, M.V. Lomonosov Moscow State University, 119992 Moscow, Russia

Richard B. Miles

Department of Mechanical and Aerospace Engineering, Princeton University, Princeton, New Jersey, 08544-5263

Received December 3, 2004; accepted March 4, 2005

Phase-matched four-wave mixing is demonstrated for millijoule nanosecond pulses guided by photonic bandgaps of hollow fibers with a two-dimensionally periodic cladding and a core diameter of $\sim 50 \mu\text{m}$. Raman resonances related to the stretching vibrations of water molecules inside the hollow fiber core are detected in the spectrum of the four-wave mixing signal, suggesting phase-matched coherent anti-Stokes Raman scattering in hollow photonic-crystal fibers as a convenient sensing technique for condensed-phase species adsorbed on the inner fiber walls and trace gas detection. © 2005 Optical Society of America

OCIS codes: 190.4370, 320.7140.

1. INTRODUCTION

Hollow-core photonic-crystal fibers (PCFs)^{1,2} offer new interesting options for high-field physics and nonlinear optics. Waveguide losses can be radically reduced in such fibers relative to standard, solid-cladding hollow fibers, owing to the high reflectivity of a periodically structured fiber cladding within photonic bandgaps (PBGs),²⁻⁵ allowing transmission of high-intensity laser pulses through a hollow fiber core in isolated guided modes with typical transverse sizes of 10–20 μm . Owing to this unique property, hollow PCFs can substantially enhance nonlinear-optical processes, including stimulated Raman scattering,⁶ four-wave mixing (FWM),⁷ coherent anti-Stokes Raman scattering (CARS),⁸ and self-phase modulation.⁹ Air-guided modes in hollow PCFs can support high-power optical solitons^{10,11} and allow transportation of high-energy laser pulses for technological^{12,13} and biomedical¹⁴ applications.

Several designs of hollow PCFs have been demonstrated, allowing the fiber structure and, hence, fiber dispersion and mode profiles to be adapted to a particular application. The dominating design solutions include PCFs with a two-dimensionally periodic hexagonal (honeycomb) photonic-crystal lattice, first demonstrated by Cregan *et al.*,¹ and Kagomé lattice-cladding PCFs, introduced by Benabid *et al.*⁶ The typical size of the PCF core ranges from 6 up to 20 μm . It would be interesting and important for many applications to extend the PCF architecture to hollow fibers with larger inner diameters. Such hollow PCFs would allow higher peak powers to be coupled into guided modes without irreversible damage on fiber walls. As the maximum peak power leading to no

damage of PCF walls scales as $\sim a^2$ with the fiber core radius a for given pulse duration and threshold fluence of optical breakdown, large-core hollow PCFs would suggest a valuable option for the peak-power scaling of pulse-compression, frequency-conversion, and soliton-transmission regimes in the high-intensity ultrafast optics of guided waves.

In this work, we demonstrate phase-matched FWM of millijoule nanosecond pulses in hollow PCFs with a period of the photonic-crystal cladding of $\sim 5 \mu\text{m}$ and a core diameter of approximately 50 μm . We will show that Raman-resonant FWM in large-core hollow PCFs enhances the potential of waveguide CARS in hollow fibers, demonstrated in earlier work,¹⁵ providing a convenient sensing tool for condensed-phase species adsorbed on the inner fiber walls and trace-gas detection.

2. EXPERIMENTAL TECHNIQUE AND PCF SAMPLES

Large-core-area hollow PCFs were fabricated using a standard procedure^{1,2} that involves stacking glass capillaries into a periodic array and drawing this preform at a fiber-drawing tower. Several capillaries have been omitted from the central part of the stack, to produce a hollow core of the fiber. Whereas in standard hollow PCFs the number of omitted capillaries is seven, the PCFs used in our experiments had a hollow core in the form of a regular hexagon, with each side corresponding to five cane diameters. The inset in Fig. 1 shows an image of a hollow PCF with a period of the cladding of approximately 5 μm and a core diameter of about 50 μm . The unsupported side of

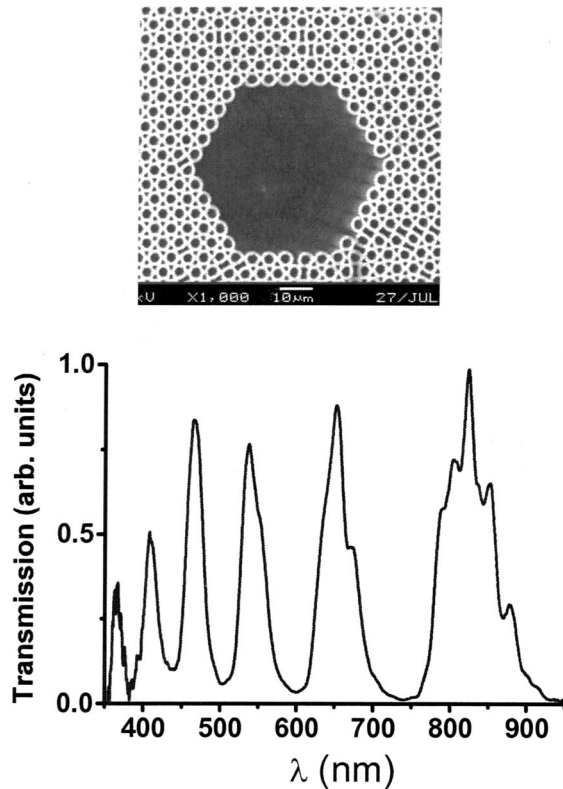


Fig. 1. Transmission spectrum of the hollow-core PCF. The inset shows the cross-section view of the PCF with a period of the cladding structure of $\sim 5 \mu\text{m}$.

the photonic-crystal structure in this fiber is much larger than that in a standard hollow PCF. The image in the inset to Fig. 1 shows, however, that this does not necessarily lead to larger nonuniformities in the transverse refractive index profile and, hence, mode-intensity profiles. The baking of capillaries forming the photonic-crystal structure, as shown in the image, allows a hollow waveguide with a nearly ideal $50\text{-}\mu\text{m}$ -diameter hexagonal core to be fabricated. It is still to be explored whether this technique can be scaled up to the fabrication of hollow PCFs with even larger core diameters. Transmission spectra of hollow PCFs employed in our experiments display well-pronounced passbands (Fig. 1), indicating the PBG guidance of radiation in air modes of the fiber.

The laser system used in our experiments consisted of a *Q*-switched Nd:YAG master oscillator, Nd:YAG amplifiers, frequency-doubling crystals, and a dye laser, as well as a set of totally reflecting and dichroic mirrors and lenses adapted for the purposes of CARS experiments. The *Q*-switched Nd:YAG master oscillator generated 15-ns pulses of $1.064\text{-}\mu\text{m}$ radiation, which were then amplified up to about 30 mJ by Nd:YAG amplifiers. A KDP crystal was used for the frequency doubling of the fundamental radiation. This second-harmonic radiation served as a pump for the dye laser, generating frequency-tunable radiation within the wavelength ranges 540–560 and 630–670 nm, depending on the type of dye used as the active medium for this laser. All three outputs of the laser system, viz., the fundamental radiation, the second-harmonic radiation, and the frequency-tunable dye-laser radiation, were employed as pump fields in FWM, as de-

scribed below. Frequency dependences of the anti-Stokes signals produced through different FWM processes were measured point by point by scanning the frequency of dye-laser radiation. The energies of these pump fields were varied in our experiments from 0.5 up to 10 mJ at the fundamental wavelength, from 0.5 to 8 mJ in the second-harmonic radiation, and from 0.05 to 0.7 mJ for the dye-laser radiation. To couple the laser fields into the fundamental mode of the PCF, we focused laser beams into spots with a diameter of $35 \mu\text{m}$ at the input end of the fiber. The PCF could withstand the energy of fundamental radiation up to 10 mJ, corresponding to a laser fluence of approximately 630 J/cm^2 , without an irreversible degradation of fiber performance because of optical breakdown. Laser-induced breakdown on PCF walls was judged by a dramatic irreversible reduction in fiber transmission and an intense sideward scattering of laser radiation, visible through the fiber cladding. While the achieved level of input energies was sufficient to produce reliably detectable FWM signals in our experiments, a further increase in the laser radiation energy coupled into the PCF is possible through a more careful optimization of the coupling geometry.

3. RESULTS AND DISCUSSION

FWM processes with the CARS-type frequency-mixing scheme $\omega_a = 2\omega_1 - \omega_2$ (ω_1 and ω_2 are the frequencies of the pump fields and ω_a is the frequency of the anti-Stokes signal produced through FWM) were studied in our experiments for two different sets of pump and signal frequencies. In the first FWM process, used in our experiments to test phase matching and to assess the influence of waveguide losses, two waves with the wavelength $\lambda_1 = 2\pi c/\omega_1$ ranging from 630 to 665 nm, provided by the dye laser, are mixed with the fixed-frequency field of the fundamental radiation at $\lambda_2 = 1064 \text{ nm}$, to generate an anti-Stokes signal within the range of wavelengths λ_a from 445 to 485 nm. The second FWM process, designed to demonstrate the potential of CARS spectroscopy with hollow PCFs, is a standard Nd:YAG-laser CARS arrangement with $\lambda_1 = 532 \text{ nm}$ and λ_2 ranging from 645 to 670 nm.

To assess the influence of phase matching and radiation losses on the intensity of the FWM signal generated in a hollow PCF, we use the result of the slowly varying envelope approximation for the power of the anti-Stokes signal^{16,17}: $P_a \propto |\chi_{\text{eff}}^{(3)}|^2 P_1 P_2^2 M$, where P_1 and P_2 are the powers of the fields with frequencies ω_1 and ω_2 , respectively; $\chi_{\text{eff}}^{(3)}$ is the effective combination of cubic nonlinear-optical susceptibility tensor components; and the factor M includes optical losses and phase-mismatch effects:

$$M(\Delta\alpha, \alpha_a l, \delta\beta l) = \exp[-(\Delta\alpha + \alpha_a)\ell] [\sin^2(\Delta\alpha/2) + \sin^2(\delta\beta/2)] [(\Delta\alpha/2)^2 + (\delta\beta/2)^2]^{-1} \ell^2,$$

where $\Delta\alpha = (2\alpha_1 + \alpha_2 - \alpha_a)/2$; α_1 , α_2 , and α_a are the magnitudes of optical losses at frequencies ω_1 , ω_2 , and ω_a , respectively, and $\delta\beta$ is the mismatch of the propagation constants of waveguide modes involved in the FWM process. To provide an estimate of 1 order of magnitude of typical coherence lengths $l_c = \pi/(2|\delta\beta|)$ for FWM processes in hollow PCFs and to choose PCF lengths L meeting the

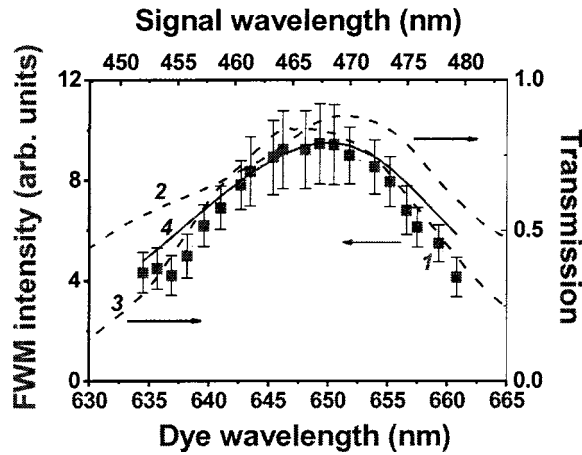


Fig. 2. Intensity of the $\omega_a=2\omega_1-\omega_2$ four-wave mixing signal from the hollow PCF with the length of 8 cm versus the wavelength of dye-laser radiation with λ_1 ranging from 630 to 665 nm and $\lambda_2=1064$ nm: 1, the measured spectrum of the FWM signal; 2, fiber transmission for dye-laser radiation; 3, fiber transmission for the FWM signal; and 4, the spectral profile of the factor M .

phase-matching requirement $L \leq l_c$ for our experiments, we substitute the dispersion of a standard hollow fiber with a solid cladding for the dispersion of PCF modes in these calculations. As shown by earlier work on PBG waveguides,¹⁸ such an approximation can provide reasonable accuracy for mode dispersion within the central part of PBGs but fails closer to the passband edges. For the waveguide FWM process involving the fundamental modes of the pump fields with $\lambda_1=532$ nm and $\lambda_2=660$ nm, generating the fundamental mode of the anti-Stokes field in a hollow fiber with a core radius of 25 μm , the coherence length is estimated as $l_c \approx 10$ cm. On the basis of this estimate, we choose a fiber length of 8 cm for our FWM experiments. With this PCF length, effects related to the phase mismatch can be neglected as compared with the influence of radiation losses.

We experimentally tested phase matching for waveguide CARS in the PCF by scanning the laser-frequency difference $\omega_1-\omega_2$ off all the Raman resonances (with λ_1 ranging from 630 to 665 nm and $\lambda_2=1064$ nm) and using the above expression for $M(\Delta\alpha L, \alpha_a L, \delta\beta L)$ with $\delta\beta L \approx 0$ to fit the frequency dependence of the FWM signal. Dots with error bars (line 1) in Fig. 2 present the intensity of the anti-Stokes signal from hollow PCFs measured as a function of the frequency of the dye laser. Dashed curves 2 and 3 in this figure display the transmission of the PCF for dye-laser radiation and the anti-Stokes signal, respectively. Solid curve 4 presents the calculated spectral profile of the factor $M(\Delta\alpha L, \alpha_a L, 0)$. Experimental frequency dependences of the FWM signals, as can be seen from the comparison of lines 1 and 4 in Fig. 2, are fully controlled by the spectral contours of PCF passbands (lines 2 and 3), indicating that phase-mismatch effects are much less significant for the chosen PCF lengths than variations in radiation losses are.

The second series of experiments was intended to demonstrate the potential of waveguide CARS in a hollow PCF for the sensing of Raman-active species. For this purpose, the frequency difference of the second-harmonic and dye-laser pump fields was scanned through the Ra-

man resonance, $\omega_1-\omega_2=2\pi c\Omega$, with O—H stretching vibrations of water molecules, adsorbed on the inner PCF walls. The frequencies Ω of O—H stretching vibrations of water molecules typically fall within a broad frequency band of 3200–3700 cm^{-1} . The frequency dependence of the FWM signal from the PCF deviates substantially from the spectral profile of the factor $M(\Delta\alpha L, \alpha_a L, 0)$ (see lines 1 and 4 in Fig. 3), clearly indicating the contribution of Raman-active species to the FWM signal. To differentiate between the CARS signal related to water molecules adsorbed on the PCF walls from the OH contamination of the PCF cladding, we measured the spectrum of the CARS signal from a PCF heated above a burner. Heating by 30 K during 30 min reduced the amplitude of the Raman resonance in the spectrum of the CARS signal by a factor of about 7. The high level of the CARS signal was then recovered within several days. This spectrum of the CARS signal from the dry PCF was subtracted from the CARS spectrum recorded at the output of the hollow PCF under normal conditions. The difference spectrum was normalized to the spectral profile of the factor $M(\Delta\alpha L, \alpha_a L, 0)$. The result of this normalization is shown by line 5 in Fig. 3.

Notably, the contrast of the experimental wavelength dependence of the FWM intensity (squares with error bars) in Fig. 2 is higher than the contrast of a similar dependence for the CARS signal in Fig. 3. This variation in the ratio of the maximum amplitude of the nonlinear signal correlates well with the behavior of transmission for dye-laser radiation and the nonlinear signal, shown by curves 2 and 3 in both figures. With the dye-laser radiation wavelength set around 650 nm, both the pump and nonlinear signal wavelengths λ_1 and λ_a in Fig. 2 are close to the respective maxima of PCF transmission. The CARS signal, on the other hand, is detected away from the maximum transmission for the dye-laser radiation and the nonlinear signal (Fig. 3). It is therefore important to normalize the measured CARS spectrum to the wavelength

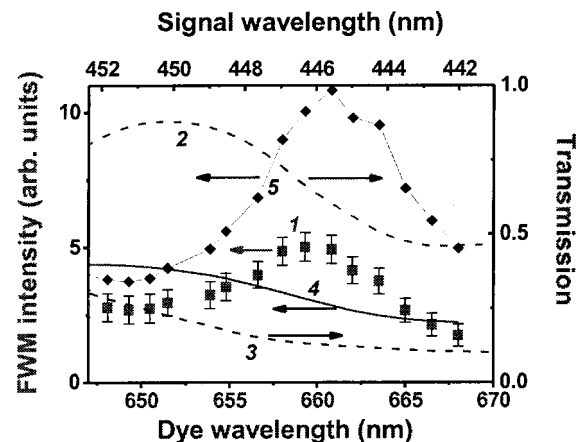


Fig. 3. Intensity of the $\omega_a=2\omega_1-\omega_2$ four-wave mixing signal from the hollow PCF with the length of 8 cm versus the wavelength of dye-laser radiation with $\lambda_1=532$ nm and λ_2 ranging from 645 to 670 nm: 1, the measured spectrum of the FWM signal; 2, fiber transmission for dye-laser radiation; 3, fiber transmission for the FWM signal; 4, the spectral profile of the factor M ; and 5, the spectrum of the FWM signal corrected for the factor M upon the subtraction of the spectrum of the CARS signal from the heated hollow PCF.

dependence of the M factor, taking into account wavelength-dependent losses introduced by the PCF. This normalization procedure considerably improves the contrast of the CARS spectrum, as shown by curve 5 in Fig. 3.

The maximum signal-to-noise ratio achieved in our CARS experiments with an 8-cm PCF (line 1 in Fig. 3) is estimated as $S/N \approx 2.9$. It is instructive to compare this ratio with a typical S/N value for CARS spectra of liquid water in a standard cell. For CARS spectra recorded with no coherent background suppression,¹⁶ the signal-to-noise ratio in CARS is controlled by the classical noise, induced by laser intensity fluctuations¹⁷: $(S/N)_{cl} \approx 2\epsilon^{-1/2} |\chi_r^{(3)}| / |\chi_{nr}^{(3)}|$, where ϵ is the mean-square deviation of laser intensity, $\chi_r^{(3)}$ is the peak value of the resonant part of the cubic nonlinear-optical susceptibility, and $\chi_{nr}^{(3)}$ is the nonresonant component of this susceptibility. With typical values of experimental parameters, $\epsilon \approx 0.02$ for our laser system and $|\chi_r^{(3)}| / |\chi_{nr}^{(3)}| \approx 0.65$ for O—H stretching vibrations¹⁶ of liquid water, we arrive at $(S/N)_{cl} \approx 9.2$. Thus CARS of water molecules adsorbed on inner PCF walls from atmospheric air under normal conditions can provide signal-to-noise ratios at the level of approximately 30% of the classical-limit signal-to-noise ratio attainable for liquid water with a standard CARS arrangement. This result suggests that CARS in hollow PCFs can be used as a convenient sensing technique for gas- and condensed-phase species filling the PCF core or adsorbed on the inner fiber walls. The signal-to-noise ratio for such a sensing technique can be radically improved through the suppression of coherent background using time-delayed pump pulses¹⁶ or coherent-control methods.¹⁹

The experiments presented above demonstrate the potential of waveguide CARS in PCFs to detect trace concentrations of Raman-active species, suggesting PCF CARS as a convenient diagnostic technique. However, CARS signals detected in these experiments do not allow the origin of Raman-active species in the fiber to be reliably identified, as it is not always possible to discriminate between the contributions to the CARS signal provided by the hollow core and PCF walls. As an example of a more easily quantifiable Raman medium, permitting the CARS signal from the PCF core to be separated from the signal from PCF walls, we chose gas-phase molecular nitrogen from atmospheric-pressure air filling the hollow core of a PCF. A two-color Raman-resonant pump field used in these experiments consisted of 15-ns second-harmonic pulses of Nd:YAG laser radiation with a wavelength of 532 nm (ω_1) and dye-laser radiation (ω_2) with the wavelength 607 nm. The dye-laser frequency was chosen in such a way as to satisfy the condition of Raman resonance $\omega_1 - \omega_2 = \Omega$ with a Q -branch Raman-active transition of N_2 at the central frequency $\Omega = 2331 \text{ cm}^{-1}$. Coherently excited Q -branch vibrations of N_2 then scatter off the second-harmonic probe field, giving rise to a CARS signal at the frequency $\omega_{CARS} = 2\omega_1 - \omega_2$ (corresponding to a wavelength of 473 nm). The hollow PCF (shown in inset 1 of Fig. 4) was designed to simultaneously provide high transmission for the air-guided modes of the second-harmonic and dye-laser radiations and the CARS signal. With an appropriate fiber structure, as can be seen from

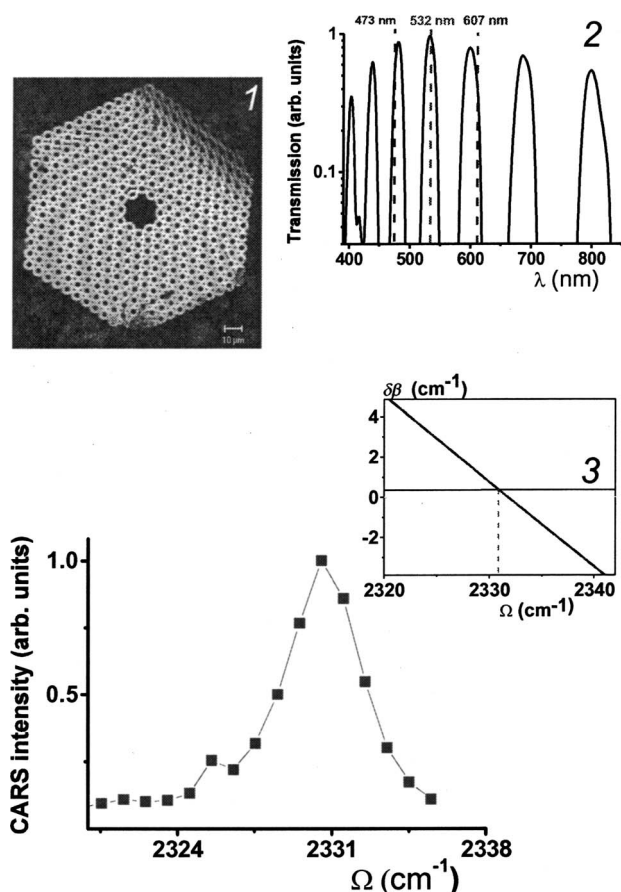


Fig. 4. CARS spectrum of Q -branch Raman-active vibrations of N_2 molecules in the atmospheric-pressure air filling the hollow core of the PCF. The insets show 1, an image of the PCF cross section; 2, the transmission spectrum of the hollow PCF designed to simultaneously support air-guided modes of the pump, probe, and CARS signal fields (their wavelengths are shown by vertical lines) in the hollow core of the fiber; and 3, the mismatch of the propagation constants $\delta\beta = 2\beta_1 - \beta_2 - \beta_a$ calculated for the $\omega_a = 2\omega_1 - \omega_2$ CARS process in fundamental air-guided modes of the hollow PCF with β_1, β_2 , and β_a being the propagation constants of the Nd:YAG-laser second-harmonic (ω_1) and dye-laser (ω_2) pump fields and the CARS signal (ω_a) in the hollow PCF.

inset 2 of Fig. 4, PCF transmission peaks can be centered around the carrier wavelengths of the input light fields and the CARS signal (shown by vertical lines in inset 2 of Fig. 4). Phase matching for CARS with the chosen set of wavelengths has been confirmed²⁰ (inset 3 of Fig. 4) by a numerical analysis of PCF dispersion based on a modification of the field-expansion technique developed by Poladian *et al.*²¹

The resonant CARS signal related to Q -branch vibrations of N_2 in these experiments can be reliably separated from the nonresonant part of the CARS signal originating from the PCF walls. The spectra of the CARS signal at the output of the PCF (Fig. 4) are identical to the N_2 Q -branch CARS spectrum of the atmospheric air¹⁶ measured in the tight-focusing regime. In view of this finding, the CARS signal can be completely attributed to the coherent Raman scattering in the gas filling the fiber core with no noticeable contribution from the nonlinearity of PCF walls.

4. CONCLUSION

We have shown in this work that large-core-area hollow PCFs bridge the gap between standard, solid-cladding hollow fibers and hollow PCFs in terms of effective guided-mode areas, allowing energy-fluence scaling of phase-matched waveguide FWM of laser pulses. We used hollow PCFs with a core diameter of $\sim 50 \mu\text{m}$ to demonstrate phase-matched FWM for millijoule nanosecond laser pulses. An intense CARS signal has been observed from stretching vibrations of water molecules inside the hollow fiber core, suggesting CARS in hollow PCFs as a convenient sensing technique for pollution monitoring and trace-gas detection. Hollow PCFs have been shown to offer much promise as fiber-optic probes for biomedical Raman applications, suggesting a method to substantially reduce the background related to Raman scattering in the core of standard biomedical fiber probes.²²

A. M. Zheltikov is the corresponding author; his e-mail address is Zheltikov@phys.msu.su.

ACKNOWLEDGMENTS

We are grateful to A. V. Shcherbakov and L. A. Melnikov for fabricating fiber samples and to D. A. Sidorov-Biryukov and E. E. Serebryannikov for useful discussions and help. This study was supported in part by the President of Russian Federation Grant MD-42.2003.02, the Russian Foundation for Basic Research (projects 03-02-16929, 04-02-81036-Bel2004, 04-02-39002-GFEN2004, and 03-02-20002-BNTS-a), and INTAS (projects 03-51-5037 and 03-51-5288). The research described in this publication was made possible in part by Award RP2-2558 of the U.S. Civilian Research and Development Foundation for the Independent States of the Former Soviet Union (CRDF).

REFERENCES

1. R. F. Cregan, B. J. Mangan, J. C. Knight, T. A. Birks, P. St. J. Russell, D. Allen, and P. J. Roberts, "Single-mode photonic bandgap guidance of light in air," *Science* **285**, 1537–1539 (1999).
2. P. St. J. Russell, "Photonic crystal fibers," *Science* **299**, 358–362 (2003).
3. S. O. Konorov, A. B. Fedotov, O. A. Kolevatova, V. I. Beloglazov, N. B. Skibina, A. V. Shcherbakov, and A. M. Zheltikov, "Waveguide modes of hollow photonic-crystal fibers," *JETP Lett.* **76**, 341–345 (2002).
4. G. Bouwmans, F. Luan, J. C. Knight, P. St. J. Russell, L. Farr, B. J. Mangan, and H. Sabert, "Properties of a hollow-core photonic bandgap fiber at 850 nm wavelength," *Opt. Express* **11**, 1613–1620 (2003).
5. C. M. Smith, N. Venkataraman, M. T. Gallagher, D. Muller, J. A. West, N. F. Borrelli, D. C. Allan, and K. Koch, "Low-loss hollow-core silica/air photonic bandgap fibre," *Nature* **424**, 657–659 (2003).
6. F. Benabid, J. C. Knight, G. Antonopoulos, and P. St. J. Russell, "Stimulated Raman scattering in hydrogen-filled hollow-core photonic crystal fiber," *Science* **298**, 399–402 (2002).
7. S. O. Konorov, A. B. Fedotov, and A. M. Zheltikov, "Enhanced four-wave mixing in a hollow-core photonic-crystal fiber," *Opt. Lett.* **28**, 1448–1450 (2003).
8. A. B. Fedotov, S. O. Konorov, V. P. Mitrokhin, E. E. Serebryannikov, and A. M. Zheltikov, "Coherent anti-Stokes Raman scattering in isolated air-guided modes of a hollow-core photonic-crystal fiber," *Phys. Rev. A* **70**, 045802 (2004).
9. S. O. Konorov, D. A. Sidorov-Biryukov, I. Bugar, D. Chorvat Jr., D. Chorvat, E. E. Serebryannikov, M. J. Bloemer, M. Scalora, R. B. Miles, and A. M. Zheltikov, "Limiting of microjoule femtosecond pulses in air-guided modes of a hollow photonic-crystal fiber," *Phys. Rev. A* **70**, 023807 (2004).
10. D. G. Ouzounov, F. R. Ahmad, D. Muller, N. Venkataraman, M. T. Gallagher, M. G. Thomas, J. Silcox, K. W. Koch, and A. L. Gaeta, "Generation of megawatt optical solitons in hollow-core photonic band-gap fibers," *Science* **301**, 1702–1704 (2003).
11. F. Luan, J. C. Knight, P. S. J. Russell, S. Campbell, D. Xiao, D. T. Reid, B. J. Mangan, D. P. Williams, and P. J. Roberts, "Femtosecond soliton pulse delivery at 800 nm wavelength in hollow-core photonic bandgap fibers," *Opt. Express* **12**, 835–840 (2004).
12. S. O. Konorov, A. B. Fedotov, O. A. Kolevatova, V. I. Beloglazov, N. B. Skibina, A. V. Shcherbakov, E. Wintner, and A. M. Zheltikov, "Laser breakdown with millijoule trains of picosecond pulses transmitted through a hollow-core photonic-crystal fibre," *J. Phys. D* **36**, 1375–1381 (2003).
13. J. D. Shephard, J. D. C. Jones, D. P. Hand, G. Bouwmans, J. C. Knight, P. S. J. Russell, and B. J. Mangan, "High energy nanosecond laser pulses delivered single-mode through hollow-core PBG fibers," *Opt. Express* **12**, 717–723 (2004).
14. S. O. Konorov, A. B. Fedotov, V. P. Mitrokhin, V. I. Beloglazov, N. B. Skibina, A. V. Shcherbakov, E. Wintner, M. Scalora, and A. M. Zheltikov, "Laser ablation of dental tissues with picosecond pulses of 1.06- μm radiation transmitted through a hollow-core photonic-crystal fiber," *Appl. Opt.* **43**, 2251–2256 (2004).
15. R. B. Miles, G. Laufer, and G. C. Bjorklund, "Coherent anti-Stokes Raman scattering in a hollow dielectric waveguide," *Appl. Phys. Lett.* **30**, 417–419 (1977).
16. S. A. Akhmanov and N. I. Koroteev, *Methods of Nonlinear Optics in Light Scattering Spectroscopy* (Nauka, 1981) (in Russian).
17. G. L. Eesley, *Coherent Raman Spectroscopy* (Pergamon, 1981).
18. S. G. Johnson, M. Ibanescu, M. Skorobogatiy, O. Weisberg, T. D. Engeness, M. Soljacic, S. A. Jacobs, J. D. Joannopoulos, and Y. Fink, "Low-loss asymptotically single-mode propagation in large-core OmniGuide fibers," *Opt. Express* **9**, 748–779 (2001).
19. N. Dudovich, D. Oron, and Y. Silberberg, "Single-pulse coherently controlled nonlinear Raman spectroscopy and microscopy," *Nature* **418**, 512–514 (2002).
20. S. O. Konorov, A. B. Fedotov, E. E. Serebryannikov, V. P. Mitrokhin, D. A. Sidorov-Biryukov, and A. M. Zheltikov, "Phase-matched coherent anti-Stokes Raman scattering in isolated air-guided modes of hollow photonic-crystal fibers," *J. Raman Spectrosc.* **36**, 129–133 (2005).
21. L. Poladian, N. A. Issa, and T. M. Monro, "Fourier decomposition algorithm for leaky modes of fibres with arbitrary geometry," *Opt. Express* **10**, 449–454 (2002).
22. J. T. Motz, M. Hunter, L. H. Galindo, J. A. Gardecki, J. R. Kramer, R. R. Dasari, and M. S. Feld, "Optical fiber probe for biomedical Raman spectroscopy," *Appl. Opt.* **43**, 542–554 (2004).